

Supplemental information

**FBP17-mediated finger-like membrane
protrusions in cell competition
between normal and RasV12-transformed cells**

Tomoko Kamasaki, Yumi Miyazaki, Susumu Ishikawa, Kazuya Hoshiba, Keisuke Kuromiya, Nobuyuki Tanimura, Yusuke Mori, Motosuke Tsutsumi, Tomomi Nemoto, Ryota Uehara, Shiro Suetsugu, Toshiki Itoh, and Yasuyuki Fujita

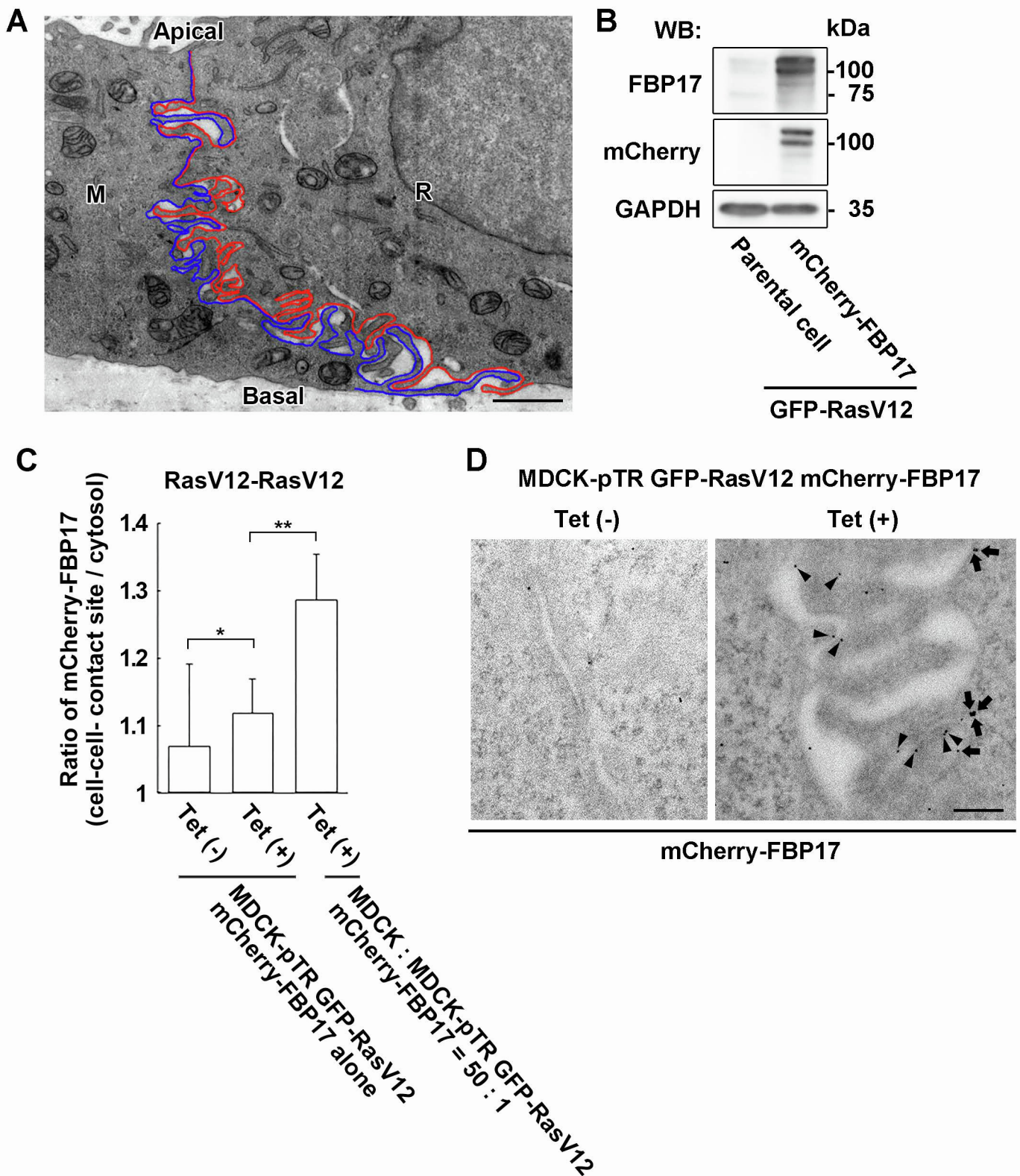


Figure S1. FBP17 is localized at wavy cell membranes (Related to Figures 1 and 2). (A) The X-Z EM image of the interface between normal and RasV12-transformed MDCK cells. Cell membranes of normal and RasV12 cells at cell-cell contacts are colored in blue and red, respectively. Scale bar, 1 μ m. (B) Establishment of MDCK-pTR GFP-RasV12 cells stably expressing mCherry-FBP17. Cell lysates were analyzed by western blotting with the indicated antibodies. (C) Quantification of the ratio of mCherry-FBP17 fluorescence (cell-cell contact site/cytosol) between MDCK-pTR GFP-RasV12 mCherry-FBP17 cells. MDCK-pTR GFP-RasV12 cells stably expressing mCherry-FBP17 were cultured alone or mix-cultured with normal cells in the absence or presence of tetracycline for 16 h. The analysis corresponds to Figure 2A. Data are mean \pm SD. * P < 0.05, ** P < 0.01 (unpaired two-tailed Student's t -tests). (D) Immuno-EM images of mCherry-FBP17 at the intercellular region between MDCK-pTR GFP-RasV12 mCherry-FBP17 cells in the absence or presence of tetracycline. Cells were fixed at 16 h after the induction of RasV12 and sectioned along the X-Y axis. The arrowheads and arrows indicate gold particles localized along and at the base of the intercellular protrusions, respectively. Scale bar, 0.2 μ m.

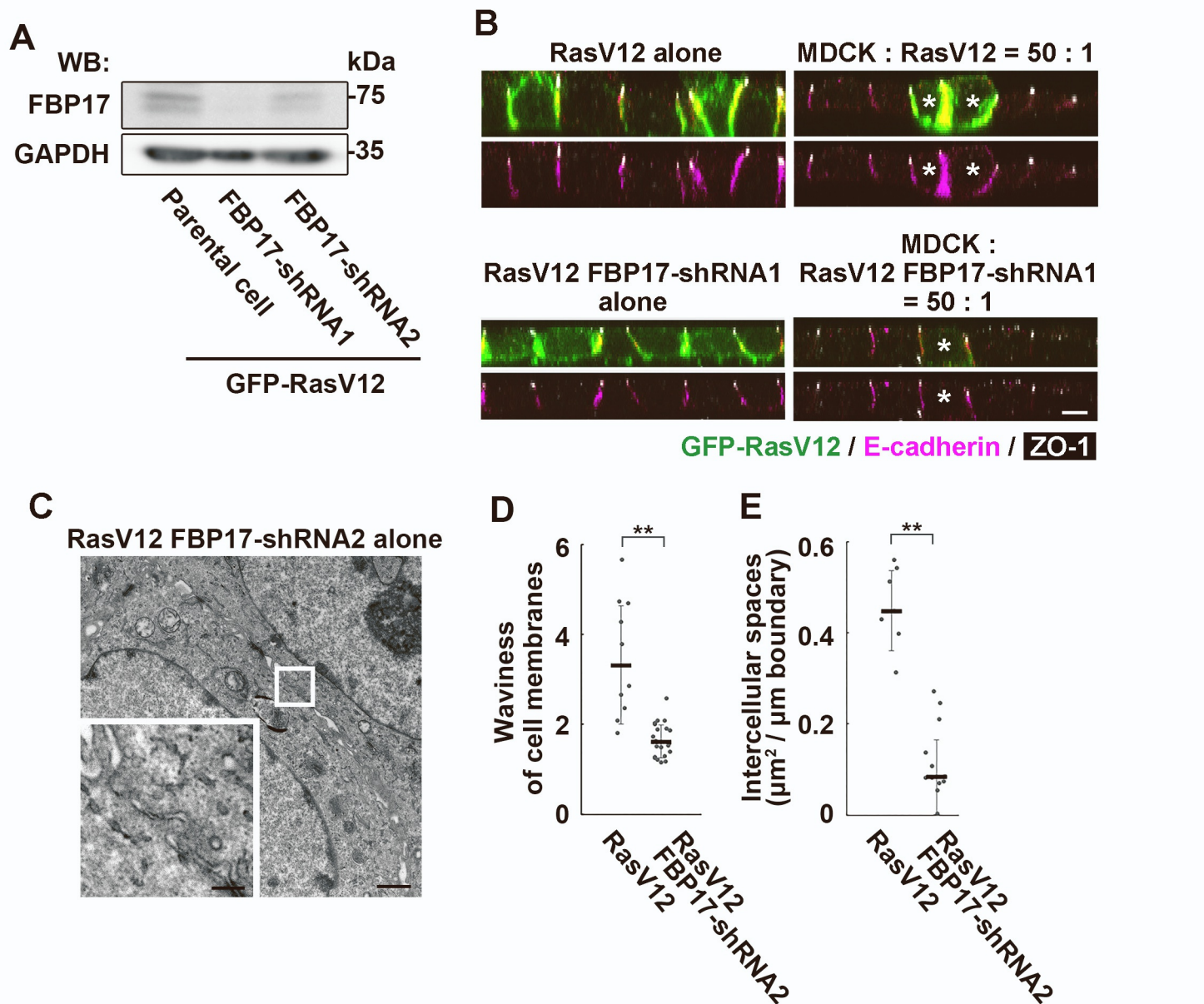


Figure S2. FBP17 in RasV12 cells regulates the formation of finger-like membrane protrusions (Related to Figure 3).

(A) Establishment of MDCK-pTR GFP-RasV12 cells stably expressing FBP17-shRNA1 or 2. Cell lysates were analyzed by western blotting with the indicated antibodies. (B) Immunofluorescence images showing single or mix cultures of RasV12 or FBP17-knockdown RasV12 cells surrounded by normal cells. Asterisks represent RasV12 or RasV12 FBP17-shRNA1 cells in the mix culture. Scale bar, 10 μm . (C) EM images of RasV12 cells stably expressing FBP17-shRNA2. Cells were fixed at 24 h after the induction of RasV12. The area in the white box is shown as inset at higher magnification, demonstrating the intercellular region. Scale bars, 1 μm ; 0.2 μm (inset). (D, E) Quantification of waviness of cell membranes (D) and intercellular spaces (E) in RasV12 cells or RasV12 FBP17-shRNA2 cells. Note that the results are comparable to Figures 3B and 3C for RasV12 FBP17-shRNA1. Data are median \pm SD. **P < 0.01 (unpaired two-tailed Student's *t*-tests).

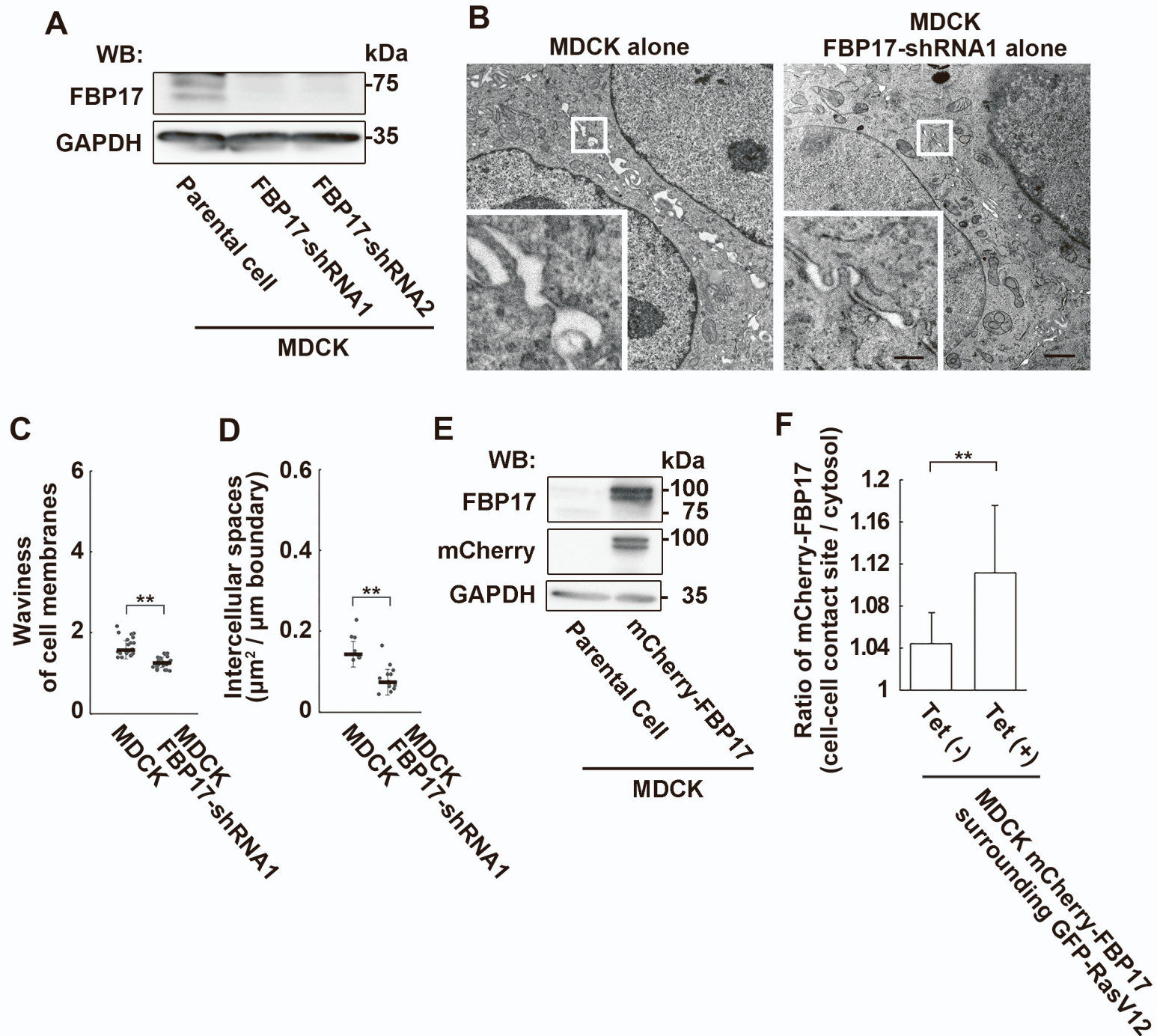


Figure S3. FBP17 accumulates at cell-cell contacts in normal cells surrounding RasV12 cells (Related to Figures 3 and 5). (A, E) Establishment of MDCK cells stably expressing FBP17-shRNA1 or 2 (A) or mCherry-FBP17 (E). Cell lysates were analyzed by western blotting with the indicated antibodies. (B) EM images of MDCK cells or MDCK cells stably expressing FBP17-shRNA1. Cells were fixed at 16 h after the addition of tetracycline. The area in the white box is shown as inset at higher magnification, demonstrating intercellular regions. Scale bars, 1 μm ; 0.2 μm (inset). (C, D) Quantification of waviness of cell membranes (C) and intercellular spaces (D) in MDCK cells or MDCK FBP17-shRNA1 cells. Data are median \pm SD. ** $P < 0.01$ (unpaired two-tailed Student's *t*-tests). (F) Quantification of the ratio of mCherry-FBP17 fluorescence (cell-cell contact site/cytosol) at the boundary between MDCK mCherry-FBP17 cells that surround MDCK-pTR GFP-RasV12 cells. Cell boundaries between the first and second row of the surrounding MDCK mCherry-FBP17 cells were analyzed. Cells were cultured in the absence or presence of tetracycline for 16 h. Data are mean \pm SD. ** $P < 0.01$ (unpaired two-tailed Student's *t*-tests)The analysis corresponds to Figure 5B.

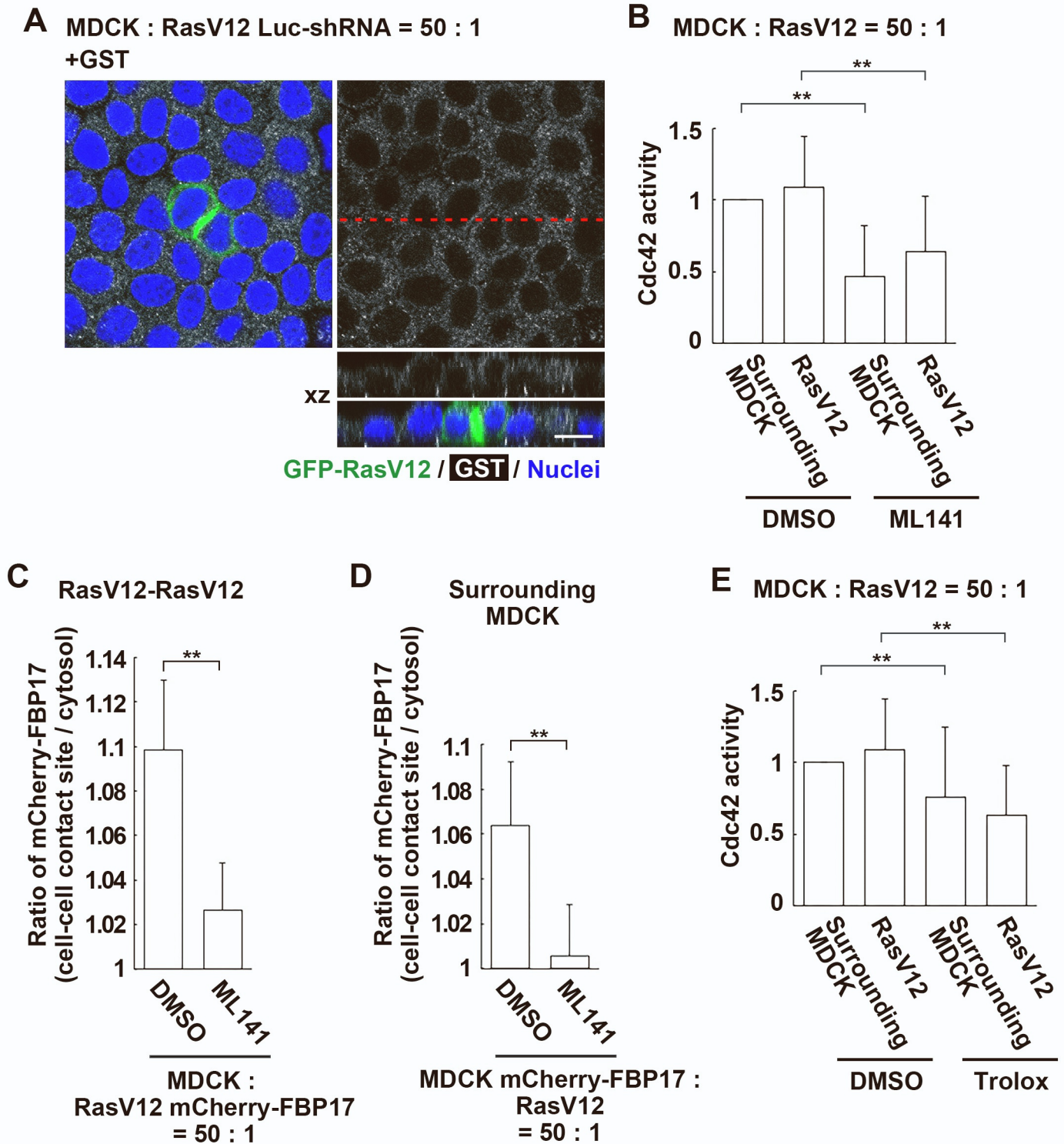


Figure S4. Indirect-immunofluorescence analysis for Cdc42 activity (Related to Figure 6). (A) Negative control for *cdc42* activity assay in mix culture of normal and RasV12-transformed cells. At 16 h after the induction of RasV12, cells were treated with GST proteins and then stained with anti-GST antibody. RasV12 cells stably expressing Luc-shRNA were used as control for RasV12 FBP17-shRNA1 cells. Scale bar, 10 μ m. (B, E) Quantification of the *cdc42* activity in mix cultures of normal and RasV12-transformed cells in the absence or presence of the *cdc42* inhibitor ML141 (B) or the antioxidant Trolox (E). Values of pixel intensity in the cytoplasm were measured and expressed as a ratio relative to Surrounding MDCK. Differences of pixel intensity between GST-WASP-CRIB and GST were calculated in each condition. (C, D) Quantification of the ratio of mCherry-FBP17 fluorescence (cell-cell contact site/cytosol) at the boundary between MDCK and MDCK-pTR GFP-RasV12 mCherry-FBP17 cells (C) or MDCK mCherry-FBP17 and MDCK-pTR GFP-RasV12 cells (D). Cells were cultured in the presence of DMSO or ML141 and tetracycline for 16 h. The analyses correspond to Figures 6C and 6D, respectively. (B-E) Data are mean \pm SD. ** $P < 0.01$ (unpaired two-tailed Student's *t*-tests).

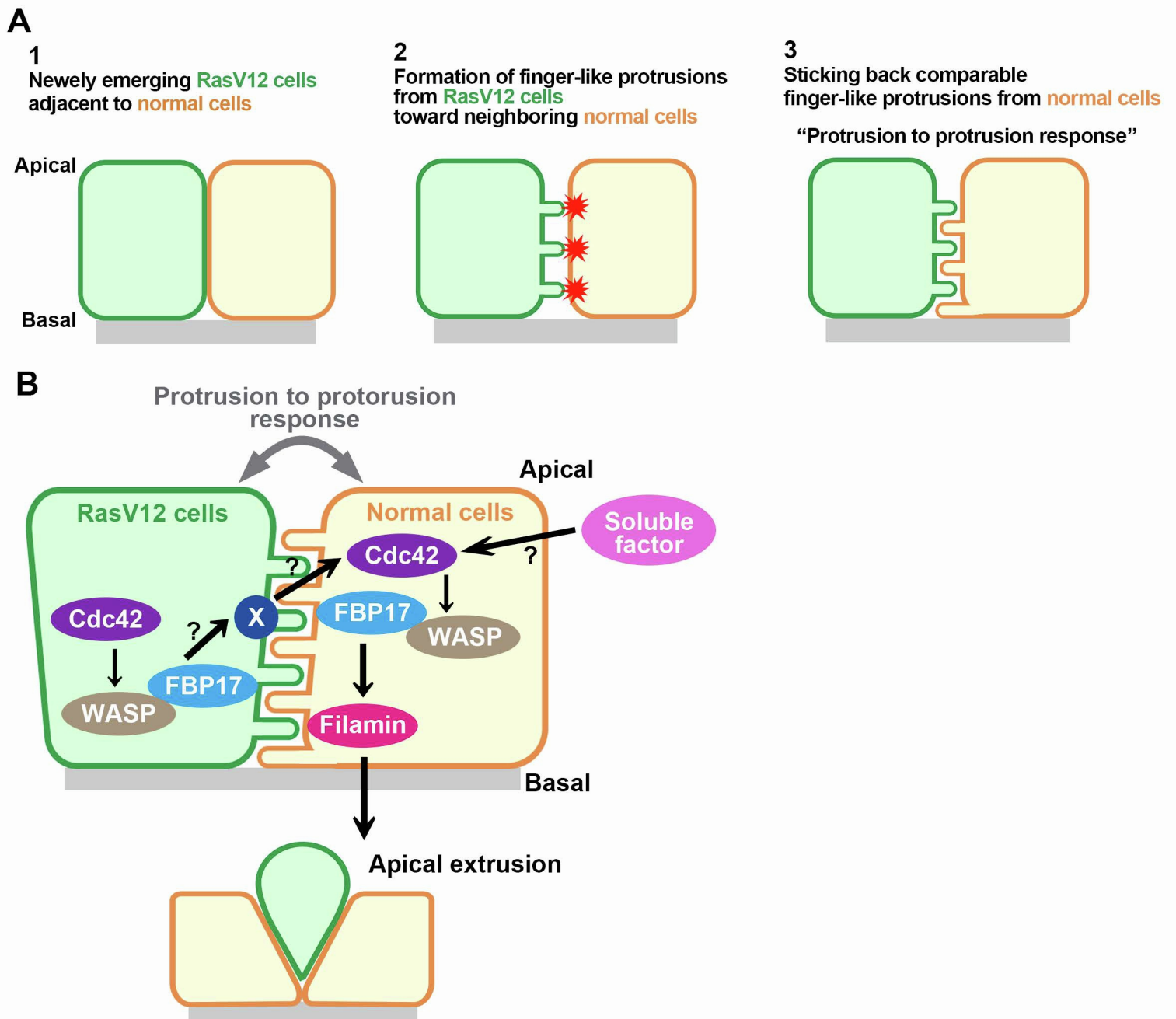


Figure S5. Molecular mechanisms of apical extrusion of RasV12-transformed cells (Related to DISCUSSION).

(A) A schematic model for ‘protrusion to protrusion response’ between normal and RasV12-transformed cells. First, RasV12-transformed cells emerge within the epithelial layer adjacent to normal cells (1). RasV12-transformed cells form finger-like membrane protrusions toward the neighboring normal cells at their cell-cell contact sites (2). Then, normal cells somehow sense the protrusions and respond to them by sticking back comparable finger-like membrane protrusions (3). (B) Schematics for molecular mechanisms of apical extrusion of transformed cells via cdc42/FBP17-mediated protrusions.